Nuclear Instruments and Methods in Physics Research A 624 (2010) 476–481

Contents lists available at ScienceDirect

Nuclear Instruments and Methods in Physics Research A

journal homepage: www.elsevier.com/locate/nima

A new concept for a cryogenic amplifier stage

V. Fedl [a,c,*], L. Barl [c], G. Lutz [b], R. Richter [a,d], L. Strüder [a,c]

[a] Semiconductor Laboratory of the Max-Planck Institutes, Otto-Hahn-Ring 6, 81739 München, Germany
[b] PNSensor GmbH, Römerstrasse 28, 80803 München, Germany
[c] Max-Planck Institute of Extraterrestrial Physics, Giessenbachstrasse, 85740 Garching, Germany
[d] Max-Planck Institute of Physics, Föhringer Ring 6, 80805 München, Germany

ARTICLE INFO

Available online 9 April 2010

Keywords:
BIB detector
DEPFET
Clear mechanism
Cryogenic conditions
Electric field enhanced emission

ABSTRACT

The observation of astrophysical objects in the mid-infrared requires Blocked Impurity Band (BIB) detectors based on n-doped Silicon. It is desirable to observe faint astronomical objects with such a detector, which can be achieved with a high signal to noise ratio. These detectors operate at a temperature range from 6 to 12 K. We foresee a new detector concept for the readout of the generated signal charge. Our aim is to implement a Depleted P-channel Field Effect Transistor (DEPFET) Active Pixel Sensor (APS) on the BIB detector in order to have a high sensitivity. We successfully operated the DEPFET under cryogenic conditions and investigated the reset mechanism of the collected signal charge.

We identified uncomplete clear with freeze-out of the signal charge into ionized shallow donor states in the heavily doped internal Gate of the DEPFET due to low thermal energy. Therefore, we found a solution to emit these localized signal charges into the conduction band in order to ensure the transport from the internal Gate to the Clear contact. It is possible to apply electric fields higher than 17 kV/cm at the position of the collected signal charge to emit the electrons from the shallow donor states. The electric field enhanced emission is equivalent to the tunneling effect.

1. Introduction

The BIB detector ranks among the advanced infrared sensors in terms of noise. This makes it an ideal detector for detection of signals from faint astrophysical objects in the infrared regime. Existing BIBs are connected via bump bonds to the first amplification stage and a readout noise of $10e^-$ ENC can be obtained [1,2]. The disadvantage of the first amplification stage is the presence of interconnection stray capacitance, which contributes to the readout noise. The aim is to develop a BIB detector which suppresses the readout noise to a minimum. This can be achieved by processing the DEPFET on top of the blocking layer of the BIB. The DEPFET goes back to the invention of Kemmer and Lutz [3]. A noise of $2.2e^-$ ENC with DEPFET at room temperature has been measured [4].

Successful characteristic measurements of the transistor, a p-channel MOSFET on top of a high resistive bulk material, were performed [5]. As well, we can measure a ^{55}Fe spectrum at temperatures down to 6 K and distinguish between the K_α- and K_β−line. Furthermore, we experimentally verified the basic properties of a sensor, which means the generation, collection and the readout of the signal charge.

The clear process is one of the crucial points to prevent internal gate overflow and furthermore, to be free of reset noise. At room temperature the clear efficiency is determined by the voltage level at the Clear and Cleargate [6]. Under cryogenic conditions, below 40 K, it is not possible to remove the signal charge by only switching the Clear and Cleargate. This paper describes a new method for the reset of linear structured DEPFETs.

Sections 2 and 3 briefly describe the BIB and the DEPFET detector concept. In Section 4 we illustrate the experiment where we operate the DEPFET and apply the new clear technique. This technique is modeled physically with the electric field assisted emission from the shallow donor states which is reported in Section 5. Furthermore, we calculated the electric fields with the simulation program, Two dimensional Semi-Conductor Analysis package (TeSCA) [7]. Section 6 discusses the experimental results considering simulations with TeSCA. The simulations show an unambiguous behavior in terms of the experimental results. Finally, we conclude the work in the final section.

2. The BIB detector

The BIB detector represents an advancement of the common extrinsic photodetector [8] in terms of higher quantum efficiency and broader wavelength response. Both detector types exploit the

* Corresponding author at: Semiconductor Laboratory of the Max-Planck Institutes, Otto-Hahn-Ring 6, 81739 München, Germany.
E-mail address: vpf@hll.mpg.de (V. Fedl).

0168-9002/$ - see front matter © 2010 Elsevier B.V. All rights reserved.
doi:10.1016/j.nima.2010.03.122

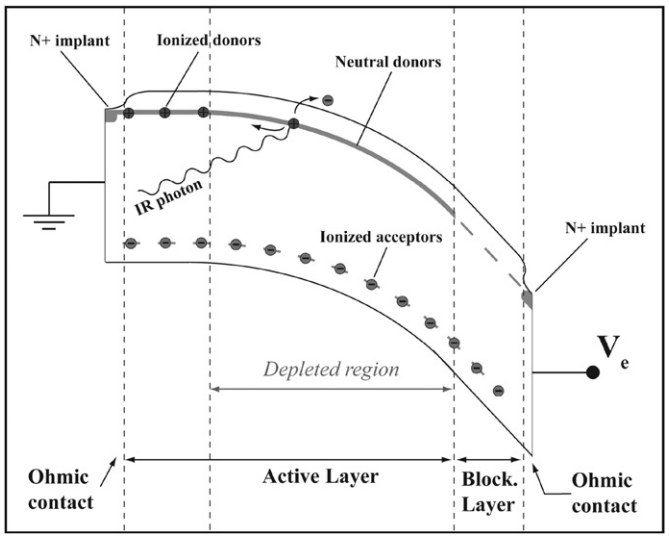

Fig. 1. Energy band structure of a BIB detector.

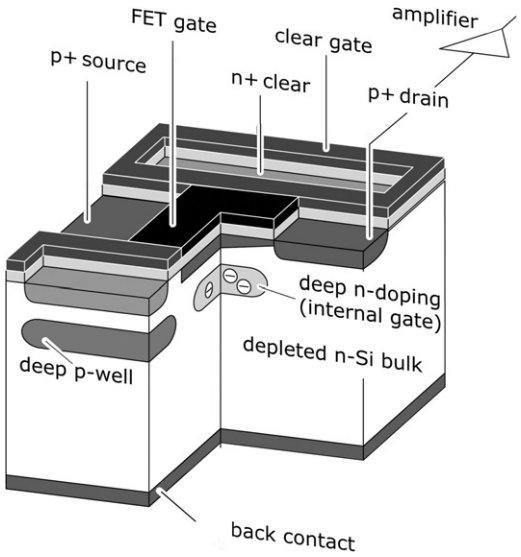

Fig. 2. Schematic cross-section of a DEPFET pixel.

excitation of the electrons by infrared radiation from the shallow donor state (binding energy: 42–54 meV) into the conduction band. Fig. 1 shows the energy band structure of the BIB detector. In comparison of extrinsic photodetectors, Si-BIB detectors are heavily doped (from $N_D = 10^{17} - 10^{18}\,1/\mathrm{cm}^3$) to have a higher absorption coefficient [9]. The high n-doping of the BIB detector results in an impurity band which is a conducting band even at low temperatures. To prevent the leakage current from this impurity band a high-resistive epitaxial (blocking) layer is grown on the heavily doped Silicon active layer. By applying a voltage V_e the active layer is depleted over several microns. Only the excited electrons within the depleted width are driven by the electric field and can pass the blocking layer to the first readout node. The aim is to introduce an integrated amplifier on the BIB detector as the first readout node with the DEPFET being a promising candidate.

3. The DEPFET

The term DEPFET refers to a structure consisting of a p-channel field effect transistor, which is integrated on the surface of a high-resistivity, n-type silicon bulk (Fig. 2). By making use of the principle of sideward depletion, the bulk can be completely depleted, and by applying appropriate potentials, a potential minimum for electrons can be generated, which is located beneath the channel of the FET. The presence of any kind of charge within this potential minimum has an influence on additional charge carriers in the transistor channel, thus modifying its electrical conductivity. Consequently, the presence of charge in the potential minimum has the same effect as the presence of charge on the transistor Gate. Therefore, the potential minimum can be considered as an internal Gate, while the "classical" Gate of a DEPFET is called external Gate for distinction.

If incoming ionizing radiation generates electron–hole-pairs within the fully depleted silicon bulk, the charge carriers are separated by the electric field, and, while the holes drift towards the p+ contact on the back surface, the electrons are collected in the closest potential minimum i.e. internal Gate. The resulting change in the channel conductivity can be used to sense the presence of charge in the corresponding internal Gate after converting it to a voltage or current signal. In this way, a DEPFET structure works as a detector for ionizing radiation. The difference of the signal before and after removing the charge from the internal Gate is now recorded. The charge is removed by a so-called clear structure, which serves as a gateable electron sink. In order to get the optimized noise performance and prevent baseline shift as well as internal Gate overflow, the electrons collected in the internal Gate must be completely removed by a clear pulse after an integration cycle. At room temperature this can be realized by applying a sufficiently high voltage on the Clear and Cleargate [10]. Under cryogenic conditions, at temperatures lower than 40 K, we additionally pulse the Source during the clear time.

4. The experiment

4.1. The measurement setup

We investigated a single pixel DEPFET which is embedded in a linear structured minimatrix of 32×24 pixels at temperatures down to 6 K. The advantage of linear DEPFETs is the direct punch-through of the Clear to the internal Gate. This is important for the reset at cryogenic temperatures. Instead, in circular structured DEPFETs, the Drain, a shallow p+ implantation, is a barrier for the collected signal electrons during the clear process. The Drain shields the Clear from a direct punch-through to the whole internal Gate and therefore, makes it inapplicable for the operation at cryogenic temperatures. At room temperature the electrons in the internal Gate diffuse and can circumvent the Drain easily. Accordingly, circular structured DEPFETs are ideal for X-ray spectroscopy as the pixel size is $75\,\mu\mathrm{m} \times 75\,\mu\mathrm{m}$ and can be easily embedded in a Silicon Drift Detector (SDD). The basic form of the Silicon Drift Detector (SDD) was proposed in 1983 by Gatti and Rehak [11].

The DEPFET chip is adhered on the ceramic, which is mounted in the cryostat and has contact to the temperature reservoir of 4.2 K. The bottom is cooled with liquid helium. To achieve higher temperatures the chip on the ceramic can be heated up by driving a current through the heat resistance, which is fixed at the mounting next to the hybrid. The temperature is determined at the mounting with a Cernox (CX-SD) thin film resistance cryogenic temperature sensor from Lakeshore. It is controlled by a feedback loop between the measured temperature at the mounting and the amount of dissipated power of the heat resistance. The mounting is made of stainless steel to prevent

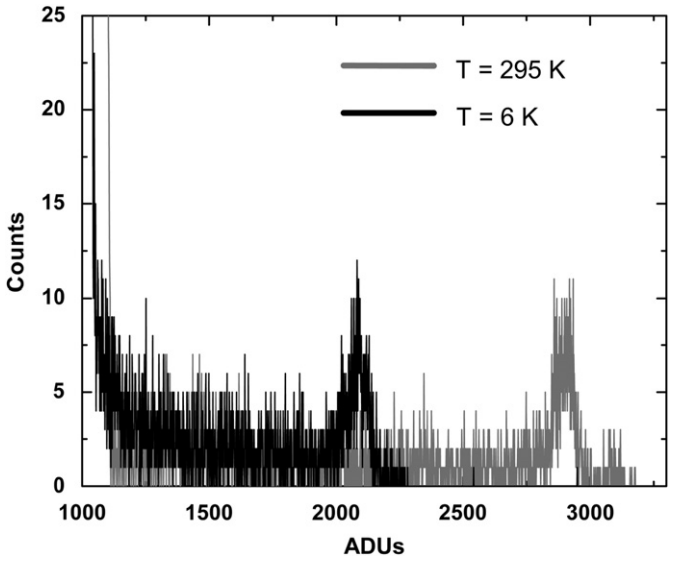

Fig. 3. ^{55}Fe spectrum of the DEPFET at room temperature and at 6 K.

heat flow to the temperature reservoir of 4.2 K and the evaporation of the liquid helium. We used stainless steel as a bad thermal conductor because of the easy implementation. The cooling from room temperature to cryogenic temperatures lasts two days and occurs via two cooling steps. In the first step the bottom is cooled down to liquid nitrogen (77.2 K) and in the second step liquid helium (4.2 K) is used. Equilibrium is achieved when the temperature at the mounting is constant at 6 K.

The frontend electronics for the single pixel chip is outside of the cryostat. The first amplifier stage of the electronics is a current–voltage converter, whose input is connected to the Drain contact of the DEPFET [12]. The Source–Drain voltage V_{SD} is held constant, so the change of the channel conductivity is connected with the change of the current. The sensor is irradiated with X-rays originating from an ^{55}Fe source to generate free signal charges in the bulk. Fig. 3 shows a ^{55}Fe spectrum of the DEPFET at room temperature and at 6 K. It is possible to distinguish between the K_α and K_β at low temperatures. We conclude that free electrons are generated by incident X-ray photons. In addition, these electrons are collected in the internal Gate of the DEPFET and they can be readout by the p-channel MOSFET. For the reset we apply the source-pulse technique.

4.2. A new clear technique

It was shown that a ^{55}Fe spectrum with the DEPFET can be obtained at temperatures down to 6 K by sampling at the beginning and the end of the integration time [5]. The difference of the two sample values is the signal level. This is independent of the fill level of electrons in the internal gate and consequently to the clear performance.

The clear process is one of the crucial points to prevent internal gate overflow and furthermore, to be free of reset noise. It is desirable to perform Correlated Double Sampling (CDS) which requires a complete clear. For CDS, the drain current is sampled before the clear pulse and immediately after clearing the pixel. In this case the empty internal Gate is the reference for the signal level.

At room temperature the clear efficiency is determined by the voltage level at the Clear and Cleargate [13]. Under cryogenic conditions, below 40 K, it is not possible to remove the signal charge by only switching the Clear and the Cleargate. The origin is the freeze-out of the signal charge into the shallow donor states of the depleted region of the internal Gate. They can be released by applying high electric fields at these localized states to emit them into the conduction band. The physical mechanism of this technique is described in Section 5. During the clear time, we pulse the Source to generate a sufficient high electric field at the position of the collected charge in order to release them from the shallow donor states into the conduction band (Fig. 4).

5. Model

The pulse scheme, which is described in Section 4.2, is the reason for the improved clear efficiency. We found out, that the potential minimum in the internal Gate changes its position, when the Source is pulsed. The collected electrons are exposed to an electric field, which forces them to emit from the shallow donors into the conduction band. Therefore, we use the simulation program TESCA to compute the potential distribution and electric fields in the internal Gate of the DEPFET. Electric fields give information about the emission times. TESCA solves the Poisson equation and the continuity equation by using the finite element method and was programmed for room-temperature applications. For the accuracy of the results for cryogenic temperatures we have to make several assumptions.

5.1. Assumptions

1. *Fully depleted internal Gate*: The device is fully depleted, which means that the donors are completely ionized. The potential is defined by the concentration of the positively charged ionized donors, which is in the range of about $N_D^+ = 10^{16}\,1/\mathrm{cm}^3$ in the internal Gate. So, we assume that the internal Gate is empty, unless signal charge arrives.
2. *Small signal assumption*: We irradiate the DEPFET with X-ray photons originating from a ^{55}Fe-source. The amount of signal charge of a single event is at most 1600 electrons, which corresponds to a free carrier concentration in the internal gate of about $n = 10^{11}\,1/\mathrm{cm}^3$. The carrier concentration was computed by calculating the time-dependent carrier concentration, when a charge cloud of 1600 electrons is generated in the bulk. The charge cloud drifts to the internal Gate, which is the global potential minimum for one pixel. This concentration lies below the ionized donor concentration in the internal Gate, which is in the range of $10^{16}\,1/\mathrm{cm}^3$. Consequently, the potential is not influenced by the incoming signal charge.

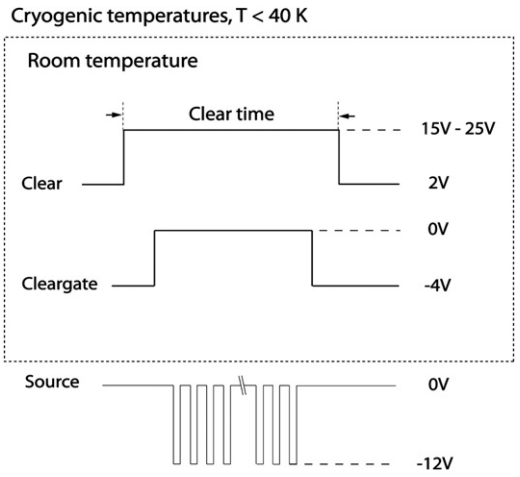

Fig. 4. The pulse schemes of the Clear and Cleargate for room temperature and cryogenic applications are shown.

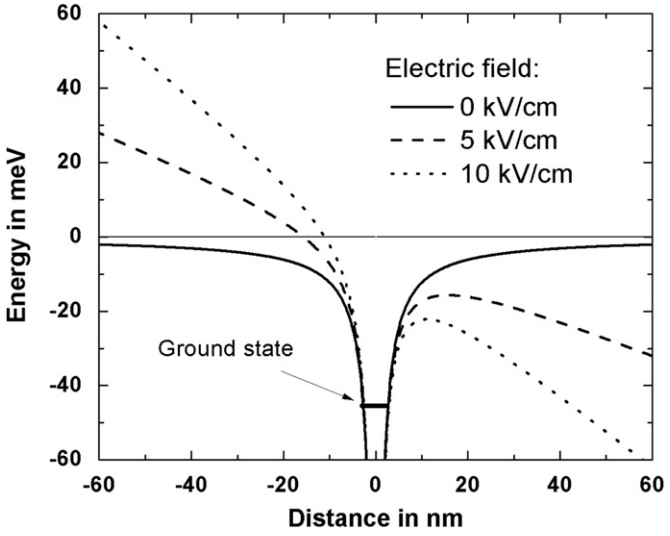

Fig. 5. The potential of a single shallow donor state at different electric fields.

3. *Recombination in the internal gate*: The internal Gate is the global potential minimum for electrons of one pixel in the device. At temperatures lower than 40 K the shallow donors represent microscopic potential minima with a binding energy of E_b=45.7 meV. These represent recombination centers, in which the electrons can be trapped.

For the recombination time τ_r we obtain

$$\tau_r = \frac{1}{\sigma v_{th} N_D^+} = 10\,\text{ps} \tag{1}$$

where $v_{th} = \sqrt{k_b T/m^*} = 1.8 \times 10^6\,\text{cm/s}$ is the thermal velocity at T=6 K, m^* is the effective mass of electrons of Silicon and N_D^+ is the density of ionized shallow donors and is $10^{16}\,1/\text{cm}^3$. For the effective mass we use $0.26m_0$, where m_0 is the mass of a free electron. The capture cross-section at 6 K is $\sigma = 2 \times 10^{-11}\,\text{cm}^2$ [14]. Below 40 K the thermal energy is not sufficient to emit the electrons in the same time constant into the conduction band.

From Eq. (1) the recombination time lies below the integration time of the detector which is in the range of microseconds. The time between readout and the clear pulse is also in the range of nano- to micro-seconds. This is related to the freeze out of free charge carriers and is experimentally shown in Ref. [5].

5.2. Electric field enhanced emission

The physical mechanism to emit the electrons from the trapped state is done by applying high electric fields at the position of the collected signal charge. The model concerns the electric field enhanced emission of trapped charge carriers from the shallow donor states into the conduction band at cryogenic temperatures.

The potential of a shallow donor state can be modeled with the hydrogen atom and can be described by the function $V(r) = -q^2/4\pi\varepsilon_0\varepsilon_r r - |\vec{E}|r$ (Fig. 5). At higher electric fields the barrier height and width of the potential are lowered. This leads to electric field enhanced emission. Here, we discuss the electric field and temperature dependent emission rate.

The thermal emission rate ε_{th} from an impurity state into the conduction band is given by [15]

$$\varepsilon_{th} = \sigma \cdot v_{th} \cdot N_C \exp(-E_b/k_b T) \tag{2}$$

with N_C being the effective density of states in the conduction band and E_b being the binding energy of the shallow donor state, which is 45.7 meV. When an electric field $|\vec{E}|$ is applied, the potential barrier is lowered by E_{PF}, so that an electron with an energy located between $E_b - E_{PF}$ and E_b is considered to be in the conduction band (Fig. 5). This is well-known and is called the Poole–Frenkel effect [16]. The reduction of the barrier is calculated by

$$E_{PF} = 2q\sqrt{\frac{q|\vec{E}|}{\varepsilon}} \tag{3}$$

with q being the unit charge, $|\vec{E}|$ the absolute value of the electric field and ε the dielectric permittivity. The electrons see a barrier which is reduced by E_{PF} and thus, enhance the thermal emission. Eq. (2) is modified to

$$\varepsilon_{PF} = \varepsilon_{th} \exp(E_{PF}/k_b T). \tag{4}$$

Furthermore, the electric field changes the barrier width between the localized state and the conduction band. This leads to the tunneling of the electrons into the conduction band. The equation for tunneling can be formulated by [17]

$$\varepsilon_{TU} = \frac{U}{6\hbar}\left(\frac{U}{E_b}\right)^2 \exp\left\{\frac{E_b}{U}^{3/2}\left[1-\left(\frac{E_{PF}}{E_b}\right)^{5/3}\right]\right\} \tag{5}$$

where $U = (3q\hbar|\vec{E}|/4\sqrt{2m^*})^{2/3}$, q is the elementary charge and $\hbar$ is the Plancks constant. The total emission time $\tau_e = 1/\varepsilon_{PF} + \varepsilon_{TU}$ is plotted against the electric field in Fig. 6. At lower electric fields the emission is dominated by thermal excitation from the ground state into the conduction band. At higher electric fields, $|\vec{E}| > 17\,\text{kV/cm}$, the barrier width comes in the range of nanometers. The electron wave function of the ground state overlaps the conduction band. This results in tunneling into the conduction band. The emission time is in the range of microseconds and is comparable to the applied clear times. Consequently, the clear efficiency can be improved.

6. Results and discussion

For calibration we use an ^{55}Fe-source. We calculate the current amplification per electron g_q of the DEPFET, which can be

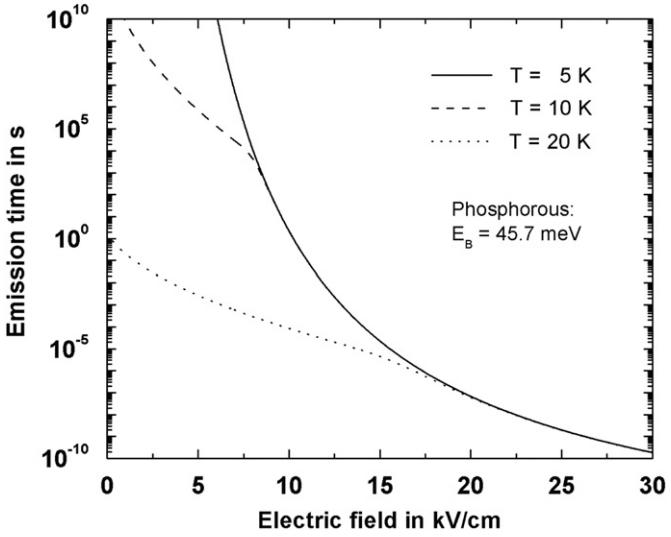

Fig. 6. Emission time against the electric field for different temperatures.

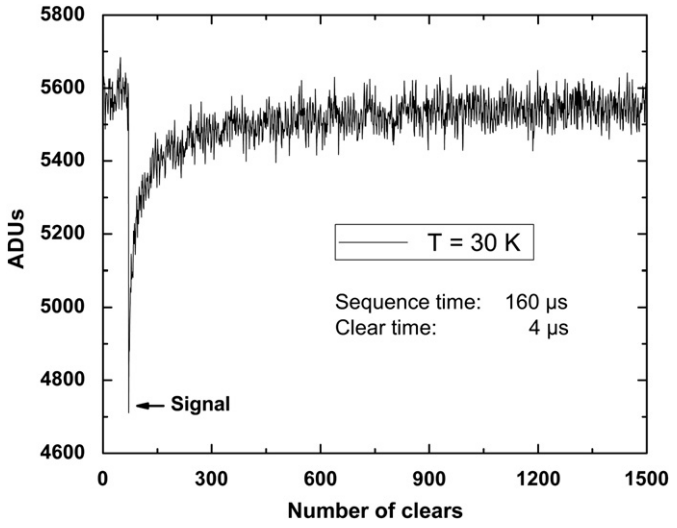

Fig. 7. Output voltage of the DEPFET of one sample during integration in ADUs in dependence of the number of clear sequences.

determined from the location of the K_α−Peak in the spectrum:

$$g_q = \frac{X_{K_\alpha} - X_R}{\frac{E_{K_\alpha}}{3.6\,\mathrm{eV}}} \frac{1}{f \cdot g} \tag{6}$$

with X_{K_α} being the position of the K_α−Peak and X_R the position of the noise peak in ADU. f is the amplification of the current–voltage converter in V/A, g is the resolution of the ADC in ADU/V and $E_{K_\alpha} = 5890\,\mathrm{eV}$ is the energy of the K_α−Peak.

The amount of the removed electrons N_{e^-} from the internal Gate after one clear pulse can be calculated by

$$N_{e^-} = \frac{\Delta V}{g_q \cdot f \cdot g} = \frac{E_{K_\alpha}}{3.6\,\mathrm{eV}} \frac{\Delta V}{X_{K_\alpha} - X_R} \tag{7}$$

where ΔV is the voltage jump after one clear pulse in ADU.

Depending on the temperature, 100–100 000 of pulses are needed to remove all electrons from the internal Gate. One example is shown in Fig. 7 for $T = 30\,\mathrm{K}$. When signal electrons arrive the internal Gate, the output voltage drops to a lower voltage level. As the output voltage level reaches the baseline after several clear sequences, we conclude that we can remove only few electrons from the internal Gate after each clear pulse. Experimentally, this is identified with the freeze-out of the signal charge.

By pulsing the Source to a negative voltage the potential minimum is shifted towards the Drain as can be seen in Fig. 8. Depending on the Source voltage relative to the Drain voltage the location of the minimum is near the Source or Drain. During charge collection, when the transistor is on, $V_S = 0\,\mathrm{V}$ and $V_D = -5\,\mathrm{V}$, the electrons in the internal Gate are attracted to the more positive Source. Consequently, the potential minimum is near the Source. During the clear time, the Source is pulsed to $-12\,\mathrm{V}$, which has the consequence that the potential minimum is shifted towards the Drain. Hence, at the position of the collected charge an electric field is generated, which forces the electrons to emit from their localized state into the conduction band.

The source-pulse technique was done at different temperatures and clear times. The amount of residual electrons in the internal Gate after a certain clear sequence is the same, when one source pulse is applied as shown in Fig. 9. From the temperature dependency we conclude that the emission is dominated by tunneling effect. At the position of the collected charge a high electric field is generated, where the electrons are emitted into the conduction band. The electric field is determined by the slope

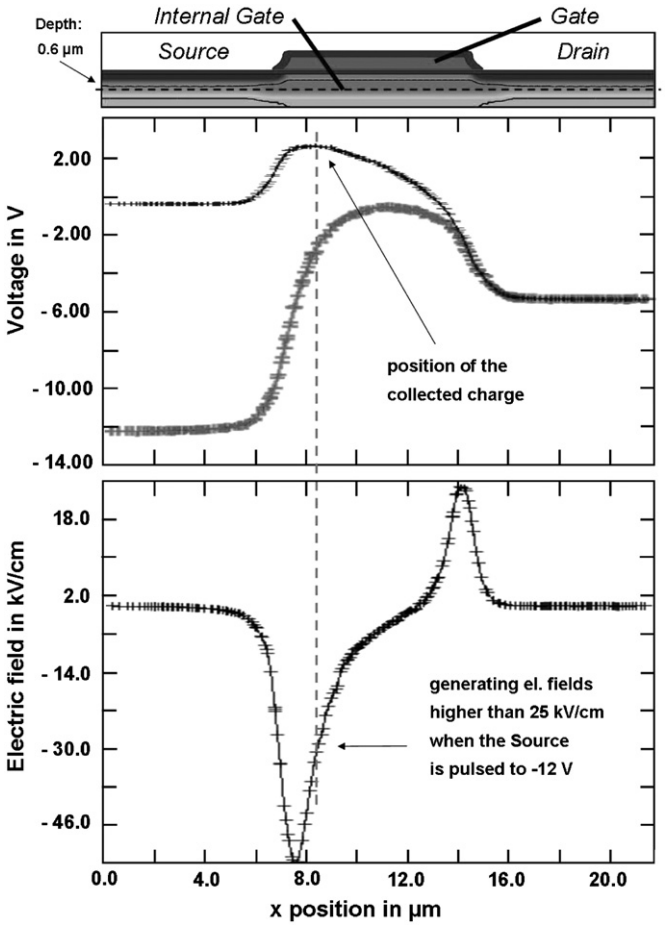

Fig. 8. Cross-section of the potential of the internal Gate at a depth of 0.6 µm in the collection state (thin curve) and in the pulsed state (thick curve). The potential maximum (potential minimum for electrons) shifts towards the Drain. Below, the electric field $E_x = \partial V/\partial x$ in the pulsed state is shown. At the position of the collected signal charge an electric field higher than 25 kV/cm is generated.

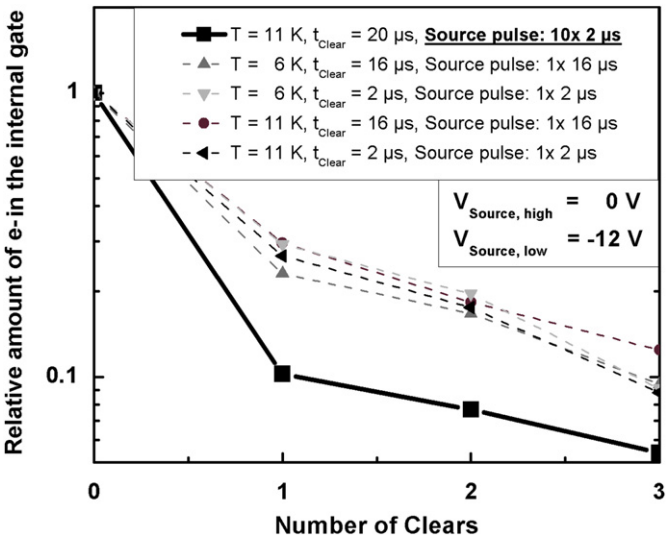

Fig. 9. The relative amount of residual signal charge in the internal Gate in dependence of numbers of clear sequences.

of the potential and is higher than 25 kV/cm (Fig. 8). From the model of electric field enhanced emission an electric field higher than 17 kV/cm is required to induce tunneling of trapped charge at temperatures lower than 20 K.

As well, the clear time is not decisive as the amount of residual electrons is the same for 2 and 16 μs. The emitted electrons drift within this electric field to the new potential minimum, which is located near the Drain. There, the electrons are trapped again. The drift time is estimated by

$$\tau_{drift} = \frac{\Delta x}{v_{drift}} = \frac{4\,\mu\text{m}}{2 \times 10^7\,\text{cm/s}} = 20\,\text{ps} \tag{8}$$

where v_{drift} is the saturation drift velocity of an electron in the conduction band at temperatures of 6–11 K [18]. Δx is the distance between the potential minima in the pulsed state and the non-pulsed state.

The recombination rate at higher electric fields can be formulated by [19]

$$R = n \cdot B_T \cdot N_D^+ \tag{9}$$

with n being the free electron concentration in the internal Gate and B_T is the capture coefficient. B_T is lower than $10^{-15}\,\text{m}^3/\text{s}$ at $|\vec{E}| > 1\,\text{kV/cm}$. Approximately 1623 electrons are generated by an incoming X-ray photon with the energy of the K_α−line. We take the spectrum of a single pixel and get a huge amount of split events. As a result, we estimate the recombination rate of 1000 electrons in the internal Gate:

$$R_{|\vec{E}|\,>\,1\,\text{kV/cm}} < 10^{10}\,\frac{1}{\text{s}}. \tag{10}$$

Consequently, the recombination time is higher than 100 ps, which is longer than the drift time calculated in Eq. (6). The whole process of emission, drift and recombination is in the range of nanoseconds, which is much smaller than the clear time:

$$\tau_{rec} + \tau_{drift} + \tau_e \approx 1\,\text{ns} \ll t_{clear} \tag{11}$$

where t_{clear} is the clear time. Consequently, the clear time, either 2 or 16 μs, does not affect the number of residual electrons. For this reason, the electrons drift from one potential minimum to another and recombine in the potential minimum. The drift time is much lower than the clear time, which causes the electrons to be trapped during the clear time and they cannot drift or diffuse to the Clear.

In the middle of the internal Gate, in-between the Cleargate, the electric field transversal to the transistor current is low. At room temperature these electrons diffuse to the Clear. Under cryogenic conditions they diffuse, while they are in the conduction band and before they are re-captured by shallow donor states in the potential minimum.

When the signal electrons arrive the internal Gate, before the first clear pulse is applied, all electrons stay in the internal Gate. After the first clear pulse, when one source pulse is applied, 20–30% of the electrons remain in the internal gate. As already discussed, this is independent of the temperature (6 and 11 K) and the clear time (2 and 16 μs). When 10 source pulses are applied, the clear efficiency can be enhanced and we reach 10% after one clear pulse. We apply 10 source pulses, each with a length of 2 μs, within one clear and observe an enhancement of the clear efficiency (Fig. 9). By applying more source pulses the reset can be enhanced. In this case, the electrons are re-emitted by pulsing the Source from −12 to 0 V generating an electric field at the position of captured electrons. They drift to the original potential minimum. Thus, the dwell time of electrons in the conduction band can be extended in order to ensure the transversal diffusion or drift to the Clear.

For future prospects, the electric field dependent recombination into ionized donors must be investigated in order to understand the diffusion and drift in the internal gate during the clear process at cryogenic conditions. This can be achieved by varying the duration and the amount of source pulses.

7. Conclusion

The DEPFET is a promising candidate for a cryogenic integrated amplifier on a Si-BIB detector. In this work the DEPFET is investigated under cryogenic conditions down to 6 K. We successfully operate the DEPFET at these temperatures and we can measure a ^{55}Fe spectrum with it. Uncomplete clear is identified with the freeze out of signal charges in the heavily doped internal gate. We found a way to remove the signal charge from the internal Gate by pulsing the Source during the clear time. This effect can be modeled with the electric field enhanced tunneling effect. Electric fields higher than 17 kV/cm at the position of the collected signal charge in the internal Gate are required to obtain emission times in the range of microseconds. By pulsing the Source several times the dwell time of the electrons in the conduction band can be extended and therefore the clear efficiency is enhanced. The experimental results are satisfactory and are unambiguous to the described model. The next step is to establish a more quantitative analysis of the reset mechanism and compute the emission, transport and recombination of the electrons in the internal Gate.

The characterization of the BIB detector in terms of quantum efficiency is necessary before we develop a BIB detector combined with an integrated DEPFET.

References

[1] M.E. Ressler, et al., Proc. SPIE 7021 (2008) 1.
[2] P.J. Love, et al., Proc. SPIE 6276 (2006) 1.
[3] J. Kemmer, G. Lutz, Nucl. Instr. and Meth. A 253 (1987) 356.
[4] M. Porro, et al., IEEE TNS 53 (2006) 401.
[5] V. Fedl, L. Barl, G. Lutz, L. Strüder, Investigation of single pixel DePMOSFETs under cryogenic conditions, in: Conference Record of IEEE Nuclear Science Symposium and Medical Imaging, vol. 1, 2008, pp. 1378–1381.
[6] C. Sandow, et al., Nucl. Instr. and Meth. A 568 (2006) 176.
[7] H. Gajewski, et al., TeSCA—Two Dimensional Semiconductor Analysis Package, Handbuch, WIAS, Berlin, 1997.
[8] A. Rogalski, Infrared Detectors, Gordon and Breach Science Publisher, 2000.
[9] M.D. Petroff, M.G. Stapelbroek, US Patent no. 4,568,960, 4 February 1986.
[10] G. Lutz, et al., Nucl. Instr. and Meth. A 572 (2007) 311.
[11] E. Gatti, P. Rehak, Nucl. Instr. and Meth. A 225 (1984) 608.
[12] S. Wölfel, et al., Sub-electron noise measurements on RNDR devices, in: Conference Record of IEEE Nuclear Science Symposium, vol. 1, 2006, pp. 63–69.
[13] C. Sandow, et al., Nucl. Instr. and Meth. A 568 (2006) 176.
[14] F.J. Morin, J.P. Maita, Phys. Rev. Lett. 30 (1973) 488.
[15] G. Lutz, Semiconductor Radiation Detectors, Springer Verlag, 1999.
[16] J. Frenkel, Tech. Phys. USSR (CAS) 5 (1938) 685;
J. Frenkel, Phys. Rev. 54 (1938) 647.
[17] E. Rosencher, V. Mosser, G. Vincent, Phys. Rev. B 29 (1984) 1135.
[18] C. Jacoboni, C. Canali, G. Ottaviani, A.A. Quaranta, Solid State Electron. 20 (1977) 77.
[19] E. Simoen, B. Dierickx, L. Deferm, C. Claeys, G. Declerck, J. Appl. Phys. 68 (1990) 4091.